Acquisition of the arginine deiminase system benefits epiparasitic Saccharibacteria and their host bacteria in a mammalian niche environment

Jing Tian[a], Daniel R. Utter[b], Lujia Cen[c], Pu-Ting Dong[c,d], Wenyuan Shi[c], Batbileg Bor[c,d], Man Qin[a], Jeffrey S. McLean[e], and Xuesong He[c,d,1]

[a]Department of Pediatric Dentistry, Peking University School and Hospital of Stomatology, National Center of Stomatology, National Clinical Research Center for Oral Diseases, National Engineering Laboratory for Digital and Material Technology of Stomatology, Beijing Key Laboratory of Digital Stomatology, Beijing 100081, China; [b]Division of Geological and Planetary Sciences, California Institute of Technology, Pasadena, CA 91125; [c]Department of Microbiology, The Forsyth Institute, Cambridge, MA 02142; [d]Department of Oral Medicine, Infection and Immunity, Harvard School of Dental Medicine, Boston, MA 02115; and [e]Department of Periodontics, University of Washington, Seattle, WA 98119

Edited by Edward DeLong, Daniel K. Inouye Center for Microbial Oceanography: Research and Education, University of Hawaii at Manoa, Honolulu, HI; received August 12, 2021; accepted November 19, 2021

Saccharibacteria are a group of widespread and genetically diverse ultrasmall bacteria with highly reduced genomes that belong to the Candidate Phyla Radiation. Comparative genomic analyses suggest convergent evolution of key functions enabling the adaptation of environmental Saccharibacteria to mammalian microbiomes. Currently, our understanding of this environment-to-mammal niche transition within Saccharibacteria and their obligate episymbiotic association with host bacteria is limited. Here, we identified a complete arginine deiminase system (ADS), found in further genome streamlined mammal-associated Saccharibacteria but missing in their environmental counterparts, suggesting acquisition during environment-to-mammal niche transition. Using TM7x, the first cultured Saccharibacteria strain from the human oral microbiome and its host bacterium *Actinomyces odontolyticus*, we experimentally tested the function and impact of the ADS. We demonstrated that by catabolizing arginine and generating adenosine triphosphate, the ADS allows metabolically restrained TM7x to maintain higher viability and infectivity when disassociated from the host bacterium. Furthermore, the ADS protects TM7x and its host bacterium from acid stress, a condition frequently encountered within the human oral cavity due to bacterial metabolism of dietary carbohydrates. Intriguingly, with a restricted host range, TM7x forms obligate associations with *Actinomyces* spp. lacking the ADS but not those carrying the ADS, suggesting the acquired ADS may also contribute to partner selection for cooperative episymbiosis within a mammalian microbiome. These data present experimental characterization of a mutualistic interaction between TM7x and their host bacteria, and illustrate the benefits of acquiring a novel pathway in the transition of Saccharibacteria to mammalian microbiomes.

Saccharibacteria | episymbiosis | arginine deiminase system | oral microbiome | TM7

The recent discovery of the Candidate Phyla Radiation (CPR), a large monophyletic radiation of phyla and superphyla that includes the group currently referred to as Patescibacteria (1) and accounts for over 26% of microbial diversity, has greatly expanded the bacterial tree of life (2–4). Among the CPR (>73 phyla), Saccharibacteria (formerly known as TM7) represents one of the only three phyla, the other two being uncultivated Candidatus Absconditabacteria and Candidatus Gracilibacteria, whose members are detected in mammalian microbiomes in addition to diverse environmental niches (5, 6). Analyses suggest multiple acquisition events (transfer of bacteria from the environment to mammals that results in stable incorporation into the mammalian microbiome) in the past led to the current wide diversity, with convergent evolution of key functions allowing Saccharibacteria from the environment with already extremely reduced genomes to adapt to mammals (7). There are six main phylogenetic groups (G1 to G6) identified within the Saccharibacteria, with only the G1 group containing both mammalian and environmental representatives. Remarkably low variation and high synteny in genomes between human-associated and groundwater Saccharibacteria have been observed for the G1 lineage, suggesting their more recent acquisition and adaptation from environmental to mammalian hosts (7). A subsequent study further suggested that other mammal-associated CPR species also originated in the environment, with the oral cavity being their most abundant habitat within animal hosts (6). Furthermore, recent studies revealed the habitat-specific difference in gene content among the CPR (5–8). Some of the highly enriched functions among mammal-associated CPR species have been implicated in either enabling use of eukaryotic host-specific resources or conferring tolerance to host-specific stressors (6). Despite these findings, the paucity of cultivated representatives has impeded the experimental evaluation of the key functions acquired by CPR species during their transition from environments to mammals.

Significance

The Candidate Phyla Radiation (CPR) is a large monophyletic lineage with poorly understood biology. Saccharibacteria are ultrasmall parasitic CPR bacteria with highly reduced genomes that have made the transition from an environmental origin to mammals. We tested the function and impact of the arginine deiminase system (ADS), an arginine catabolism pathway likely acquired by mammal-associated Saccharibacteria during their environment-to-mammal niche transition. We showed that the acquired ADS not only helped facilitate Saccharibacterial adaptation to mammals but also contributed to the establishment of cooperative episymbiotic interaction with their bacterial hosts within mammalian microbiomes. Our study provides experimental evidence demonstrating the importance of function acquired by Saccharibacteria during niche transition in facilitating their adaptation from the environment to a mammalian niche.

Author contributions: J.T. and X.H. designed research; J.T., L.C., P.-T.D., and X.H. performed research; J.T., D.R.U., W.S., B.B., M.Q., J.S.M., and X.H. analyzed data; and J.T., D.R.U., W.S., B.B., M.Q., J.S.M., and X.H. wrote the paper.

The authors declare no competing interest.

This article is a PNAS Direct Submission.

[1]To whom correspondence may be addressed. Email: xhe@forsyth.org.

This article contains supporting information online at http://www.pnas.org/lookup/suppl/doi:10.1073/pnas.2114909119/-/DCSupplemental.

Published January 6, 2022.

The first cultivated representative of Saccharibacteria and the CPR group, *Nanosynbacter lyticus* strain TM7x, was coisolated with its host bacterium *Actinomyces odontolyticus* strain XH001 (referred to as XH001 in this study) from the human oral cavity (9). TM7x has an ultrasmall cell size (200 to 300 nm), and a reduced genome of only 705 genes with limited de novo biosynthetic capabilities (9, 10). Initial characterization revealed a unique lifestyle of TM7x as an obligate epiparasite grown on the surface of its host bacterium XH001, gaining essential growth requirements at the expense of XH001 under typical laboratory conditions (10, 11). Furthermore, TM7x cells can dissociate from their host bacteria for horizonal transmission when compatible species/strains are present (11). Accumulating evidence indicates that CPR organisms have shared characteristics such as ultrasmall cell sizes, reduced genomes with minimal biosynthetic capabilities, and physical association with prokaryotic host cells, suggesting that symbiosis could be a common lifestyle shared by these diverse while phylogenetically related bacterial groups (4, 8). Cultivation of additional human oral Saccharibacteria (12) has further confirmed the generality of an obligate symbiotic lifestyle and allows the possibility of investigating the specific functions enabling their adaptation to animal-associated habitats and, more broadly, their relationship with their host bacteria.

In this study, using TM7x and its host bacterium XH001 as a model system, we experimentally investigated the functions likely acquired during the transition of Saccharibacteria from the environment and adaptation to a mammalian niche. Despite having highly reduced genomes, a complete arginine deiminase system (ADS), an arginine catabolism pathway encoded by a four-gene locus, is found in the majority of mammal/human-associated, but not environmental, Saccharibacteria strains. We show that TM7x encodes an intact and functional ADS, which allows TM7x cells to catabolize arginine, an amino acid readily available within the human oral cavity (13), and generate intermediate and final catabolites including adenosine triphosphate (ATP) and ammonia. Importantly, the ADS maintains the membrane integrity and infectivity of TM7x cells when they are dissociated from their host bacteria, thus facilitating their transmission to other host bacteria and ensuring their propagation. Furthermore, the TM7x-encoded ADS confers a shared benefit to both TM7x and its host bacterium by protecting both partners from acid stress. Intriguingly, TM7x can specifically form a symbiotic relationship with *Actinomyces* spp. lacking the ADS (including XH001) but not those carrying an ADS pathway, suggesting the ADS in TM7x may be important for TM7x–host bacteria coevolution. Our data presented experimental evidence demonstrating the benefit conferred by an acquired function (e.g., the ADS) in Saccharibacteria species that facilitates their adaptation from the environment to a mammalian niche.

Results

The ADS Is Commonly Found in Mammal/Human-Associated, But Not Environmental, Saccharibacteria. Genomic analyses across the newly uncovered diversity of the Saccharibacteria from both mammals (human oral and mammalian rumen) and the environment suggested acquisition of key genes/functions that may have allowed Saccharibacteria from the environment to adapt to mammalian hosts (7). Among those genes/functions, many of which were single genes of varying functions, a complete ADS consisting of a four-gene locus was of particular note. The ADS-encoding genes within the Saccharibacteria G1 genomes are mostly arranged in an operon containing four major genes homologous to *arcA*, *arcB*, *arcC*, and *arcD/E* (14, 15), which encode arginine deiminase (ADI), ornithine carbamoyltransferase (OTC), carbamate kinase (CK), and an arginine/ornithine antiporter, respectively. A more comprehensive comparative pangenomic analysis (Fig. 1*A* and *SI Appendix*, Fig. S1) revealed that, among the 93 currently available Saccharibacteria genome assemblies meeting completeness and quality metrics, there is a clear trend that all G1, G6, and the majority of G3 Saccharibacteria associated with mammalian rumen/human oral microbiomes carry all four ADS genes (*SI Appendix*, Fig. S1). These genes, however, were not detected in mammal-associated G5 assemblies. In contrast, only a single assembly of all the assemblies derived from environmental sources carries the complete set of four ADS genes, with the majority ($n = 53$) containing none (Fig. 1*A*). Of the three that harbor incomplete sets of ADS genes, two carry only *arcA*, and the third is missing *arcB* (Fig. 1*A* and *SI Appendix*, Fig. S1). The observed drastic difference in ADS distribution patterns suggests acquisition of this pathway by Saccharibacteria strains may confer a fitness benefit in the mammalian niche. The oral cavity contains readily available arginine both from host endogenous secretion and exogenous dietary intake (16). Thus, catabolism of arginine through an ADS pathway could generate ATP and ammonia (17), which could potentially help Saccharibacteria to adapt by providing energy as well as protection against acid stress (18).

TM7x Encodes a Complete ADS Pathway Which Is Lacking in Its Host Bacterium XH001. Since the ADS pathway carried by Saccharibacteria has not been validated or characterized, we sought to experimentally test the function and impact of the ADS in human-associated Saccharibacteria, taking advantage of our model coculture system of *N. lyticus* strain TM7x and its host bacterium XH001 (9) (Fig. 1*B*). The TM7x genome contains a cluster of four genes in the same operon which tentatively encode functions involved in the ADS pathway. BLAST searches revealed that TM7x_03440, TM7x_03435, and TM7x_03425 were homologous to genes encoding putative ADI, OTC, and CK, respectively (19), the three key enzymes involved in arginine catabolism, while TM7x_03430 encoded a putative arginine/ornithine antiporter, which facilitates the stoichiometric exchange of extracellular arginine for ornithine, an intracellular product of arginine catabolism (20) (Fig. 1 *B* and *C*).

Because the other Saccharibacteria groups (G2 to G6) lack cultivated representatives, all the available genome sequences of Saccharibacteria belonging to these groups are obtained from metagenomic studies, and most are not fully curated. Even though individual ADS genes can be detected, as shown in Fig. 1*A*, it is challenging to determine if they are in the same operon or gene order due to limitations of metagenomic genome assembly. Thus, we compared the TM7x-encoded ADS with that of Saccharibacteria HMT-350, one of the G6 oral Saccharibacteria with a better curated genome, as well as those characterized in non-Saccharibacteria species. The four-gene cluster of the ADS in TM7x displayed the same gene order as that identified in HMT-350. Meanwhile, TM7x-encoded ADI, OTC, arginine/ornithine antiporter, and CK showed the highest level of amino acid sequence identity (78, 85, 51, and 78%) to their respective counterparts in HMT-350 (Fig. 1*C*). Among the non-Saccharibacteria bacterial species, TM7x-encoded ADI, OTC, and CK displayed the highest level of amino acid sequence identity (63, 65, and 51%) to their respective counterparts in *Bacillus cereus* (Fig. 1*C*), which were encoded by *arcA*, *arcB*, and *arcC*, respectively (21). Furthermore, ADI, OTC, and CK in TM7x also showed overall moderate-level sequence identity at the amino acid level (34 to 57, 53 to 60, and 43 to 51%, respectively) to their counterparts found in human oral bacteria, including *Actinomyces johnsonii* F0510, *Lactobacillus fermentum* IFO3956, *Streptococcus pneumoniae* ATCC700669, and *Streptococcus sanguinis* SK36, albeit with varying order in gene arrangement (Fig. 1*C* and *SI Appendix*, Fig. S2 *A–C*). Intriguingly, the TM7x_03430–encoded arginine/ornithine antiporter showed a low degree of amino acid sequence identity (15%) to that of *B. cereus* ATCC14579 encoded by *arcD*, but rather displayed much

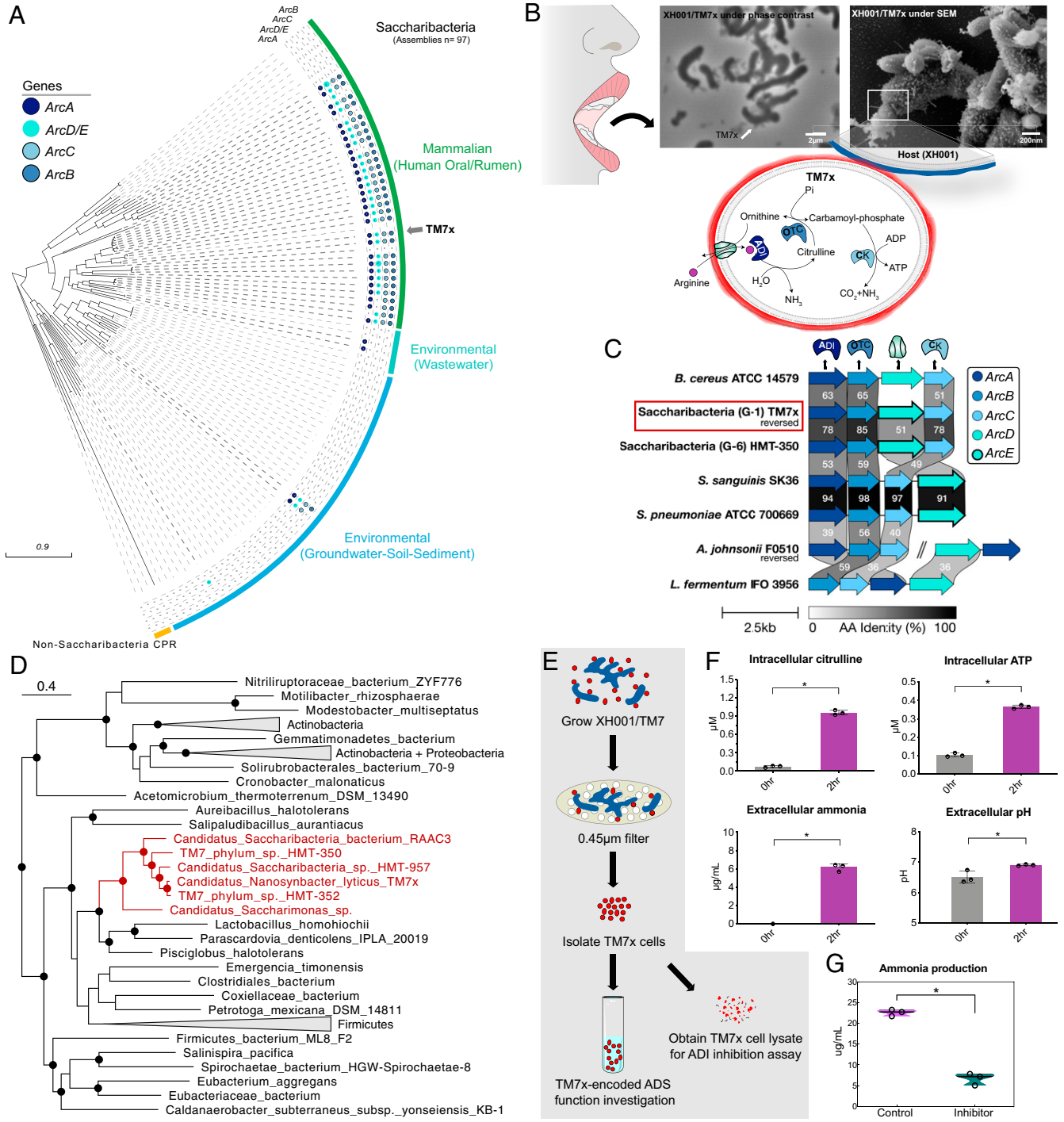

Fig. 1. ADS distribution within Saccharibacteria phyla and functional characterization of the TM7x-encoded ADS pathway. (*A*) Comparative pangenome analysis of ADS gene distribution in Saccharibacteria phyla. (*B*) TM7x (*N. lyticus* type, strain TM7x HMT-952) previously coisolated together with its host bacterium *A. odontolyticus* strain XH001 from the human oral cavity are shown in phase-contrast and scanning electron microscopy (SEM) images. The TM7x-encoded ADS pathway including one antiporter and three enzymes, namely ADI, OTC, and CK. (*C*) Comparison of the TM7x-encoded four-gene cluster of putative ADS pathway–related genes with those found in oral Saccharibacteria (G6) HMT-350, four oral bacterial species, including *A. johnsonii* F0510, *L. fermentum* IFO3956, *S. pneumoniae* ATCC700669, and *S. sanguinis* SK36, as well as *B. cereus* ATCC14579. Amino acid sequence percent identity is shown between each species. (*D*) Maximum-likelihood phylogeny of all arginine deaminase (ArcA) amino acid sequences in UniProt, clustered at 50% identity. ArcA from select Saccharibacteria (red) were readded to the 50% set. Dots mark nodes with at least 50% bootstrap support. (*E*) Experimental setup to isolate TM7x cells from XH001/TM7x coculture, and test the function of the TM7x-encoded ADS pathway, as well as obtain TM7x cell lysate for an ADI inhibitor (L-canavanine) assay. (*F*) Intracellular citrulline and ATP, and extracellular ammonia and pH, levels of prestarted TM7x cells were measured at 0 and 2 h following incubation in arginine-supplemented saline. (*G*) Ammonia was measured 2 h following enzyme-containing TM7x lysate incubation in control (L-arginine) and inhibitor (with the same concentration of L-arginine and L-canavanine) solution. Data are presented as mean values ± SD (error bars) from three biologically independent experiments; statistical analysis was carried out using Student's *t* test (unpaired, two-tailed); an asterisk indicates a significant difference between the two groups (*$P < 0.05$).

higher (43%) sequence identity to the arginine/ornithine antiporter in *S. pneumoniae*, which is encoded by *arcE* (*SI Appendix*, Fig. S2 *D* and *E*). *arcE* and *arcD* encode a functionally similar but evolutionarily unrelated arginine/ornithine antiporter (22). Thus, TM7x_03440, TM7x_03435, TM7x_03430, and TM7x_03425 were given the gene identifiers *arcA*, *arcB*, *arcE*, and *arcC*, respectively.

To investigate the evolutionary origins of the ADS pathway in Saccharibacteria in greater detail, we chose ArcA, i.e. ADI, for further analysis. ArcA is a good representative as it encodes a key enzyme in the ADS and is amenable to public database searches as it lacks known paralogs. Further, ArcA should represent the evolutionary history of the other genes for Saccharibacteria, assuming the entire locus was acquired as a complete functional unit as suggested by genomic analyses (Fig. 1 *A* and *C*). All known bacterial ArcA amino acid sequences (n = 8,892) were downloaded from UniProtKB. Sequences were clustered to 65% identity (n = 304 after reading all Saccharibacterial ArcA) and used to construct a phylogenetic tree (Fig. 1*D* and *SI Appendix*, Fig. S3). The phylogenetic arrangement of ArcA revealed that Saccharibacteria-encoded ArcA formed a monophyletic clade sister to a larger clade of several Firmicutes genera, including *Bacillus*, *Lactobacillus*, and *Staphylococcus*. Saccharibacterial ArcA was notably distant from Actinobacteria, the phylum containing all currently known hosts for extant Saccharibacteria validated through cultivation studies (Fig. 1*D*). These relationships indicate that Saccharibacteria may have ancestrally obtained their ADS via horizontal gene transfer (HGT) from an ancient Firmicutes bacterium rather than HGT from an ancestral Actinobacteria host. Within Saccharibacteria, disparities between the ArcA phylogeny and phylogenomic relationships (7) point to possible HGT among oral resident Saccharibacteria. For example, the ArcA sequences of human-associated G1 Saccharibacteria (HMT-952 [including TM7x], HMT-352, and HMT-488) were more closely related to the human-associated but evolutionarily distant G6 Saccharibacteria (HMT-350) than to non–human-associated G1 Saccharibacteria (RAAC3 and *Candidatus Saccharimonas aalborgensis*) (Fig. 1*D* and *SI Appendix*, Fig. S3).

In contrast to TM7x, genomic analysis did not identify ADS pathway–related genes in XH001. Importantly, XH001 and TM7x did not contain any urease homologs, which catalyze the hydrolysis of urea into carbon dioxide and ammonia and is another major acid tolerance system found in many oral bacteria. Therefore, the TM7x-encoded ADS seems a strong candidate for coping with acid stress in the oral cavity.

The TM7x-Encoded ADS Is Functionally Active. To investigate if the TM7x-encoded putative ADS operon is functional, TM7x cells were isolated from XH001/TM7x coculture using an established protocol (Fig. 1*E*) (11). Collected TM7x cells were washed and resuspended in 0.85% NaCl (referred to as saline) to mimic starvation conditions. TM7x cells were then further incubated in arginine-supplemented saline, a slightly modified condition that has been used for investigating oral bacterial ADS function (23, 24). The key intermediate and final catabolites of the ADS pathway, including intracellular citrulline, ATP, and extracellular ammonia concentration, as well as extracellular pH, were measured immediately and 2 h after incubation. Data showed that after starvation in saline for 24 h, the concentrations of both intracellular citrulline and ATP were close to zero, while 2-h incubation of prestarved TM7x cells in arginine-supplemented saline resulted in a significant increase in intracellular citrulline and ATP, as well as extracellular ammonia and pH (Fig. 1*F*), indicating the TM7x-encoded ADS pathway is intact and functional.

Due to its unique epiparasitic lifestyle, no genetic tools are available at this point to allow studying gene function via targeted mutagenesis in TM7x. As an alternative approach, we used a bacterial ADI enzyme inhibitor, L-canavanine, to further confirm the function of the TM7x-encoded ADS. L-canavanine is a naturally occurring L-amino acid that interferes with L-arginine–utilizing enzymes due to its structural similarity to arginine. It can serve as a slow substrate that inhibits the ADI enzyme of *B. cereus* (25). We incubated TM7x cell lysate containing ADS enzymes in arginine (control) or arginine supplemented with L-canavanine (inhibitor) solution. The ammonia concentration was measured 2 h after incubation. The results showed that when L-canavanine was present, the amount of ammonia generated was three times less than the control group (Fig. 1*G*), further confirming the involvement of the TM7x-encoded ADS pathway in observed arginine catabolism.

TM7x Maintains Higher Membrane Integrity and Infectivity in the Presence of Arginine. Considering TM7x is exceedingly metabolically restrained, we further investigated if arginine catabolism via the ADS helps maintain TM7x survival in the absence of their host bacteria. TM7x cells isolated from XH001/TM7x coculture were incubated in saline supplemented or not with arginine. The cell-membrane integrity was monitored by SYTOX Green, a high-affinity nucleic acid–binding fluorophore that only penetrates cells with compromised membranes. Compared with the no-arginine group, the presence of arginine mildly but significantly reduced the percentage of TM7x cells displaying fluorescence signal at both days 1 and 7 (Fig. 2*A*). A positive control was included which showed most if not all TM7x cells displayed fluorescence signal after 15-min treatment with Triton X-100 (Fig. 2*A*). Quantitative analysis of the fluorescence intensity measured at days 1, 2, and 7 revealed that the arginine group showed significantly lower fluorescence signal than the no-arginine group (Fig. 2*B*). Our data indicate the presence of arginine helps TM7x in maintaining membrane integrity, thus underscoring the importance of arginine catabolism for TM7x survival when disassociated from their host bacteria.

We then studied the impact of arginine on the ability of TM7x to infect new hosts, as transmission between hosts is a critical step in symbioses with impacts on host bacterial genome evolution as well as stability and long-term maintenance of these symbionts within mammalian hosts (26, 27). Isolated TM7x cells were incubated in saline supplemented or not with arginine for 24 h. The cells were then harvested to perform infection assays based on a previously published protocol (11). Briefly, TM7x cells were mixed together with XH001n, a naive XH001 strain that is sensitive to the infection of TM7x and displays a growth-crash phenotype when challenged with TM7x in successive passages, as reflected by the drop in its OD_{600} (optical density at 600 nm) and colony-forming units (CFUs) as well as the observation of branched and enlarged XH001n cells physically associated with multiple TM7x cells by phase-contrast microscopy (11). The culture of TM7x-infected XH001n will then recover from the crash and resume growth with relatively normal rod-shape morphology as the two bacteria establish a stable association (11, 28). Furthermore, the number of passages it takes for XH001n populations to crash is inversely correlated with the number of added freshly isolated TM7x cells (11, 28). Our data revealed that when TM7x cells were preincubated with arginine, they maintained higher infectivity than those incubated in the absence of arginine, as reflected by fewer passages (three vs. seven) before host populations crashed. The timing of the XH001n population crash was consistent whether using OD_{600} data, XH001n CFU measurement, or direct examination under the microscope (Fig. 2 *C* and *D*). Furthermore, when TM7x cells were incubated with arginine, they maintained much higher levels of intracellular ATP and extracellular ammonia at 24 h (Fig. 2*E*). In addition, the pH of the medium was significantly higher, likely due to the increased level of ammonia production (Fig. 2*E*). Intriguingly, while there was only a mild increase in the percentage of cells displaying compromised

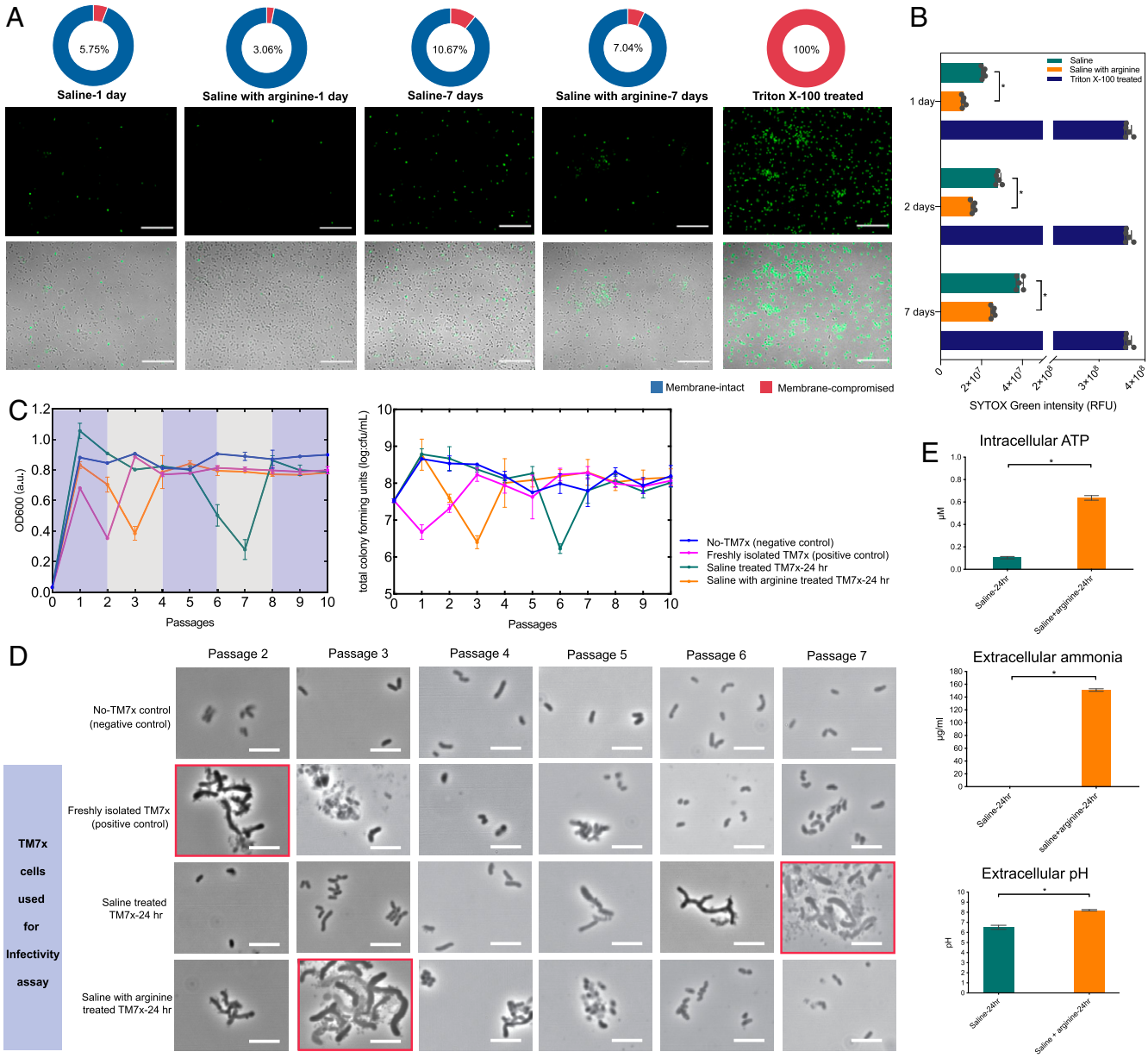

Fig. 2. TM7x maintains higher membrane integrity and infectivity via the ADS pathway. (*A*) Isolated TM7x cells were incubated in saline or saline supplemented with arginine for 1 and 7 d, or treated with Triton X-100 detergent as a positive control, and then harvested and stained with SYTOX Green. Representative images are shown as a fluorescence channel and fluorescence/transmission merged channel. (Scale bars, 10 μm.) The estimated percentage of TM7x cells with compromised membranes was estimated by calculating the value of average fluorescence intensity in each group divided by that of Triton X-100–treated samples with an equivalent total number of TM7x cells. (*B*) SYTOX Green intensity was measured 1, 2, and 7 d after incubation and quantitatively analyzed using Student's *t* test (unpaired, two-tailed); an asterisk indicates a significant difference between the two groups (*$P < 0.05$). RFU, relative fluorescence unit. (*C*) Growth crash of XH001n culture was monitored in an infectivity assay by OD_{600} and CFU of XH001n to determine the infectivity of differentially treated TM7x cells. a.u., arbitrary unit. (*D*) Phase-contrast images for each group (as in *C*) from passage 2 to passage 7. (Scale bars, 5 μm.) Images with a red box indicate XH001n cells experiencing growth crash when challenged with differentially treated TM7x cells. (*E*) Intracellular ATP, extracellular ammonia concentration, and extracellular pH levels were measured after incubating TM7x cells in saline or saline supplemented with arginine. Statistical analysis was carried out using Student's *t* test (unpaired, two-tailed); an asterisk indicates a significant difference between the two groups (*$P < 0.05$).

membranes between the arginine- and no-arginine group (5.75 vs. 3.06%) based on a similar experimental setup (Fig. 2*A*), it took an additional four passages for cells in the no-arginine group to induce crash compared with cells from the arginine group. Our previous study showed that, when using freshly isolated TM7x, >10-fold cells are required to achieve one passage faster in inducing growth crash of XH001n culture (28). Taken together, the data suggest that while the majority of the TM7x cells maintained their membrane integrity in the no-arginine group after 24 h, their infectivity was severely affected compared with TM7x cells in the arginine group.

Arginine Catabolism Improves TM7x Survival and Maintains Its Infectivity under Acid Stress. Outside TM7x, the ADS pathway has been implicated in conferring protection against acid stress through ammonia production (17). We then investigated if ADS-mediated arginine catabolism can protect TM7x from acid stress. A pH around 5 is frequently encountered within the

human oral cavity due to bacterial fermentation of dietary carbohydrates (29). Our data showed that incubation of TM7x cells in pH 5 buffer for 24 h led to a mild but significant increase in fluorescence signal compared with those incubated in pH 6 or 7 buffer when stained with SYTOX Green (Fig. 3*A*). When incubated at pH 6 and 7 for 24 h, only 5.30 and 3.97% (Fig. 3*B*), respectively, of TM7x cells displayed compromised membranes, and they were capable of inducing crash in XH001n culture at passage 3 in an infectivity assay (Fig. 3*D*). Intriguingly, while incubation in pH 5 buffer led to only a mild increase in the percentage (less than 13%) of membrane-compromised TM7x cells (Fig. 3*B*), these TM7x cells completely lost their ability to infect and induce crash in XH001n over an experimental period of 10 passages (Fig. 3 *D* and *E*). The results indicate that while most of the TM7x cells (>87%) still maintained their membrane integrity when incubated at pH 5 for 24 h, their infectivity was greatly affected. A similar trend in infectivity was observed for TM7x cells incubated for 48 h at different pHs (Fig. 3*F*).

In comparison, supplementation of arginine in pH 5 buffer led to better TM7x survival, as reflected by overall reduced fluorescence signal compared with the no-arginine control when stained with SYTOX Green (Fig. 3*G*). This is consistent with the decreased percentage (9.36%) of TM7x cells displaying fluorescence signal in arginine-supplemented compared with the no-arginine control (12.84%) (Fig. 3*H*), even when the solution pH remained constant at 5 in both treatments. Furthermore, the presence of arginine in the pH 5 buffer allowed TM7x cells to induce crash of XH001n culture at passage 4 for cells incubated for 24 h (Fig. 3 *I* and *J*) and at passage 7 for cells incubated for 48 h (Fig. 3*K*). Our result suggested that TM7x could achieve better survival and, more importantly, maintain infectivity during acid stress in the presence of arginine, likely through stabilizing intracellular pH via ADS-mediated arginine catabolism and ammonia production (30).

TM7x Protects Its Host Bacterium from Acid Stress via Arginine Catabolism. Since TM7x's host bacterium XH001 is lacking both the ADS and urease, the two common pathways to achieving pH homeostasis under acid stress (30), we further investigated if the function of the TM7x-encoded ADS could potentially protect XH001 from acid stress during their symbiotic association by increasing the pH of their microenvironment. We showed that when incubated in saline supplemented with 10 mM glucose (Fig. 4*A*), the pH dropped from 7.0 to around 5.25 after 2-h incubation and remained steady thereafter for both XH001 mono- and XH001/TM7x cocultures (Fig. 4*A*). Addition of 10 mM arginine did not affect the pH dynamics in an XH001 monoculture, but it led to a smaller pH drop (from 7 to 5.75) in XH001/TM7x coculture 2 h after incubation, followed by gradual recovery of pH to 6 after 8 h of incubation (Fig. 4*A*). Next, we investigated whether the observed diminishment of the initial pH drop and the subsequent recovery of pH in XH001/TM7x coculture supplemented with arginine was correlated with increased ammonia production. The data showed that no noticeable ammonia could be detected in either XH001 mono- or XH001/TM7x cocultures in the absence of arginine (Fig. 4*C*). In contrast, addition of arginine led to significant accumulation of ammonia in XH001/TM7x coculture but not XH001 monoculture (Fig. 4*C*). Furthermore, we observed that XH001 cells, either in monoculture (with or without arginine) or coculture (without arginine), suffered more than 3 and 6 orders of magnitude loss in CFU viability after 12- and 16-h incubation, respectively (Fig. 4 *D* and *E*). In contrast, XH001 cells in XH001/TM7x coculture supplemented with arginine maintained significantly higher viability, ~1 to 2 orders of magnitude higher than those in other groups at 12 and 16 h post incubation, respectively (Fig. 3 *D* and *E*). These data indicate that TM7x cells protect their host bacteria from acid stress by mitigating the pH drop in the microenvironment through the production of ammonia via the ADS.

TM7x Prefers *Actinomyces* spp. Lacking a Complete ADS Pathway as Host. Previous studies revealed TM7x displayed a restricted host range and was able to establish an epiparasitic relationship with a tight cluster of oral *Actinomyces* spp. closely related to XH001 (11, 12). Oral *Actinomyces* spp. largely fall into two major clades: 1 and 2 (Fig. 4*F*). Recent data showed that while clade 1 *Actinomyces* were capable of serving as TM7x hosts, species in clade 2 do not form detectable associations with TM7x (28). Intriguingly, pangenomic analysis revealed that XH001 and *Actinomyces* spp. from clade 1 lacked either the whole ADS gene cluster or *arcA*, which encodes the key ADS pathway enzyme ADI (Fig. 4*F*). In contrast, clade 2 *Actinomyces* spp. all carry *arcA*, *arcB*, and *arcC*, which encode ADI, OTC, and CK, the three key enzymes in the ADS pathway. Two *Actinomyces* spp. from clade 2, *A. johnsonii* and *Actinomyces graevenitzii*, and two from clade 1, XH001 and *Actinomyces meyeri* W712, were tested for their ammonia production via arginine catabolism. Data showed that after 24-h incubation in 10 mM L-arginine and 10 mM glucose-supplemented saline, while XH001 and *A. meyeri* W712 did not produce noticeable ammonia, both species from clade 2 generated ammonia, albeit at different levels (3 and 9 μg/mL for *A. johnsonii* and *A. graevenitzii*, respectively) (Fig. 4*G*). The detection of ammonia production indicated those ADS pathways in nonhost *Actinomyces* spp. are indeed functional. An infection assay further confirmed previous findings that while TM7x was able to infect XH001 and *A. meyeri* W712, it failed to establish symbiotic association with *A. johnsonii* and *A. graevenitzii*, the two *Actinomyces* spp. that carry a functional ADS pathway (Fig. 4*H*).

Discussion

Long considered microbial "dark matter," the CPR is a group of phylogenetically related yet genomically diverse bacteria whose evolution, lifestyle, and ecological role remain largely elusive due to their recalcitrance to cultivation (1, 2, 4). Increasing lines of evidence indicate that mammal-associated CPR, including Saccharibacteria, were ancestrally environmental, perhaps most recently acquired from groundwater sources (6, 7). Due to their obligate symbiotic lifestyle, Saccharibacteria lineages transitioning from groundwater to animal microbiomes must solve at least two problems—first, they need a suitable host bacterium in the new environment, and second, they must survive the conditions of the new environment. For the first problem, the simplest solution is that the host bacterium transitions along with the Saccharibacteria; however, it is possible that the Saccharibacteria could forge a new symbiosis with a new bacterial host in a new environment. The few experimental host-range analyses suggest that Saccharibacteria are generally not so strict as to associate with a single host strain; their host range can encompass multiple closely related bacterial species (28). Thus, if the environmental bacterial host(s) had mammal-associated congeners at the time of the transition, Saccharibacteria may have been able to more easily establish a relationship with such new but related host bacteria. The second problem, on the other hand, can most easily be solved by acquisition of relevant gene functions via HGT. HGT plays an important role in bacterial evolution (31, 32), particularly adaptive evolution, where the functions gained via HGT could facilitate bacterial adaptation to new ecological niches (33–36), including the human body (36, 37). In a recent study, we have bioinformatically characterized and reported on the type IV secretion system in TM7x, which could be potentially involved in facilitating HGT (7).

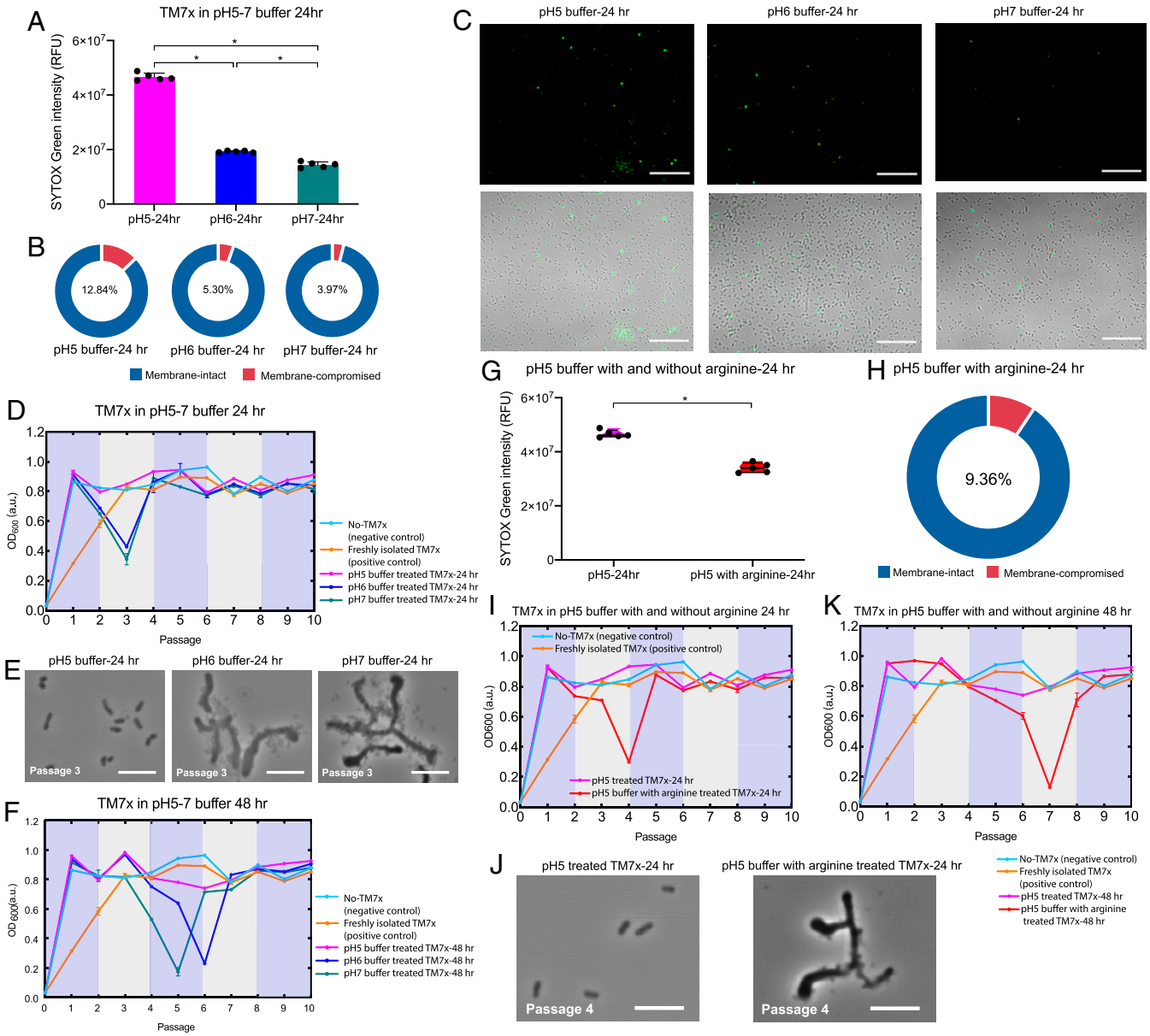

Fig. 3. Arginine improves TM7x survival and maintains its infectivity under acid stress. Isolated TM7x cells were incubated in pH 5 acetate buffer, pH 6 phosphate buffer, pH 7 phosphate buffer, and pH 5 acetate buffer supplemented with arginine for 24 and 48 h and then harvested for SYTOX Green staining and infectivity assay. (*A*) SYTOX Green intensity was measured at 24 h for the pH 5, 6, and 7 groups after incubation and quantitatively analyzed using Student's *t* test (unpaired, two-tailed); an asterisk indicates a significant difference between the two groups (*$P < 0.05$). (*B*) The estimated percentage of cells with compromised membranes was estimated by calculating the value of average fluorescence intensity in each group (as in *A*) divided by that of Triton X-100–treated samples with an equivalent total number of TM7x cells. (*C*) Representative images are shown as a fluorescence channel and fluorescence/transmission merged channel. (Scale bars, 10 μm.) (*D*) TM7x infectivity assay. Growth crash of XH001n culture was monitored by OD_{600} to determine TM7x cells' infectivity after incubating in pH 5, 6, and 7 buffer for 24 h. (*E*) Phase-contrast images of samples taken from the infectivity assay for each group at passage 3, when XH001n cells experienced a growth crash when challenged with TM7x preincubated in pH 6 and 7, but not pH 5, buffer for 24 h. (Scale bars, 5 μm.) (*F*) Infectivity assay using TM7x cells preincubated in different-pH buffers for 48 h. (*G*) SYTOX Green intensity was measured for TM7x cells incubated in pH 5 buffer supplemented with and without arginine for 24 h. Data were analyzed using Student's *t* test (unpaired, two-tailed); an asterisk indicates a significant difference between the two groups (*$P < 0.05$). (*H*) The percentage of cells with compromised membranes was estimated by calculating the value of average fluorescence intensity in each group (as in *G*) divided by that of Triton X-100–treated TM7x samples. (*I*) Infectivity assay using TM7x cells preincubated for 24 h in pH 5 buffer supplemented with and without arginine. (*J*) Phase-contrast images of samples taken from an infectivity assay (as in *I*) at passage 4 for the group using TM7x cells treated with pH 5 buffer alone (*Left*) and the group using TM7x cells treated with pH 5 buffer supplemented with arginine (*Right*). (Scale bars, 5 μm.) (*K*) Infectivity assay using TM7x cells preincubated for 48 h in pH 5 buffer supplemented with and without arginine.

The observation that ADS-encoding genes are a common feature of mammal-associated, but not environmental, Saccharibacteria (Fig. 1*A*), particularly for G1, which display preferred niches within the mammalian oral cavity (6), suggested that the ADS could be a key pathway acquired during their adaptive transition from environment to mammals. The ADS pathway catalyzes the conversion of arginine to ornithine, carbon dioxide, and ammonia, with the concomitant generation of ATP (17). In

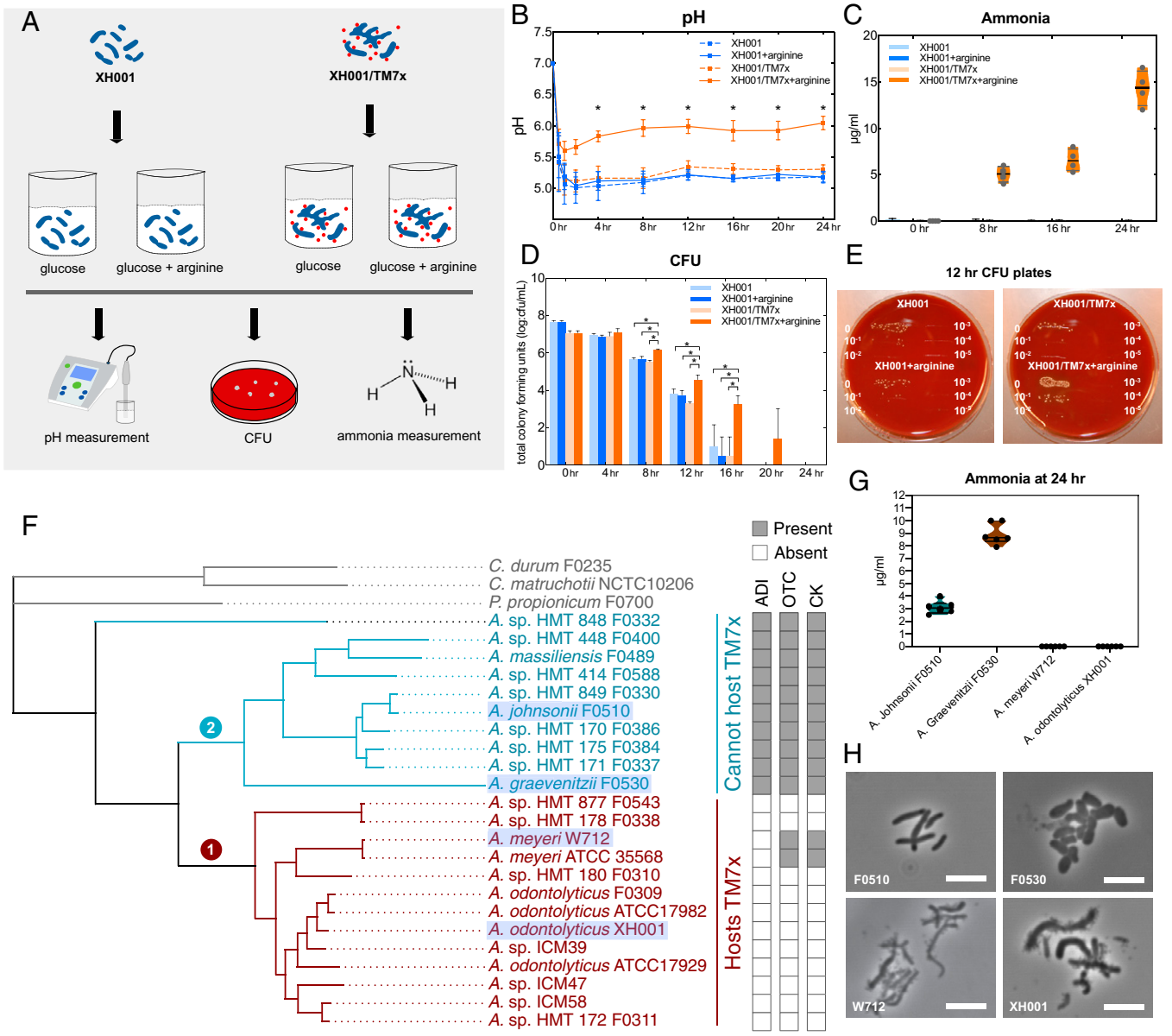

Fig. 4. TM7x-mediated pH buffering improves XH001 survival under acid stress which correlates with this strain only forming obligate associations with *Actinomyces* spp. lacking the ADS. (*A*) XH001 mono- and XH001/TM7x coculture were incubated in 0.85% NaCl + 10 mM glucose solution, supplemented with and without 10 mM arginine, a condition used for studying bacterial ADS function (23, 24). (*B*–*E*) pH of the solution (*B*), extracellular ammonia concentration (*C*), and XH001 viability (*D* and *E*) were monitored at the time points indicated (*Materials and Methods*). TM7x does not form a colony by itself. CFU data reflect only XH001 (*D* and *E*). Average values ± SD are shown. A Kruskal–Wallis test (all pairwise, Bonferroni-adjusted) was used for statistical analysis; asterisks indicate significant differences between values (*$P < 0.05$). (*F*) A phylogenetic tree was created using the 16S ribosomal RNA gene sequences of these oral *Actinomyces* spp. which revealed two clades: clade 1 (red) containing *Actinomyces* species capable of forming parasitic association with TM7x, and clade 2 (blue) including *Actinomyces* species unable to serve as host for TM7x based on experiments reported in ref. 28. The presence or absence of genes encoding the three key enzymes involved in the ADS pathway—ADI, OTC, and CK—within the genomes of these *Actinomyces* species is marked. (*G* and *H*) Two representative *Actinomyces* spp. from each clade (highlighted with light purple background) were chosen to test their ADS-mediated ammonia production (*G*) and TM7x infection (*H*). (*G*) Ammonia production after incubating *A. johnsonii* F0510, *A. graevenitzii* F0530, *A. meyeri* W712, and XH001 in saline supplemented with glucose and arginine for 24 h. (*H*) Phase-contrast images showing the non-TM7x hosts *A. johnsonii* F0510 and *A. graevenitzii* F0530, as well as the TM7x hosts *A. meyeri* W712 and XH001, during a TM7x infectivity assay. (Scale bars, 5 μm.)

addition to being a major means of energy production, the ADS has been implicated in conferring protection against acid stress through ammonia production as well as being involved in microbial pathogenicity (30, 38). Differences in pH were likely important to the transition of Saccharibacteria from environmental to mammal-associated habitats, particularly in the oral cavity. The pH of underground water typically ranges from 6 to 8.5, and is generally stable within a system (4). In contrast, the pH of the oral cavity can fluctuate drastically between 7 and 6 to <4 within a period of minutes to hours because of microbial metabolism of dietary carbohydrates (39, 40). Accordingly, many of the oral microbes possess diverse mechanisms to cope with such frequent acid stress, including the ADS (19, 30). Furthermore, the oral cavity contains readily available arginine both from host endogenous secretion and exogenous dietary intake (16). Thus, the acquisition of ADS or similar pH-modulating pathways were likely important for the successful transition of certain Saccharibacteria to mammalian habitats.

As an obligate epiparasite with limited metabolic capability, the ability of TM7x to remain viable and maintain infectivity when disassociated from the host bacterium during horizontal transmission is critical for its propagation and persistence within the human oral cavity. Our data strongly indicate that ADS-mediated arginine catabolism is important for TM7x cells to maintain infectivity under both neutral and acidic conditions. Interestingly, supplementation of arginine only mildly affected TM7x membrane integrity (Figs. 2*A* and 3*B*) but drastically impacted its infectivity (Figs. 2 *C* and *D* and 3 *I*–*K*). This could be explained by the following: 1) Membrane integrity is not a good indicator for viability in TM7x or, more likely, 2) while the majority of TM7x may stay viable in the absence of arginine, they might tend to lose their infectivity, a process that is more metabolically demanding. Furthermore, as a commensal *A. odontolyticus* species residing within the human oral cavity, XH001 is lacking both the ADS and urease, two common pathways to achieve pH homeostasis under acid stress (30). While TM7x was initially regarded as a "parasite" that negatively affects the growth of its host bacterium under laboratory conditions (9, 10), we presented experimental evidence demonstrating a benefit provided by TM7x to its host bacterium. Specifically, under laboratory conditions mimicking oral cavity acid stress, TM7x provides protection to XH001 via a TM7x-encoded ADS, highlighting the benefit conferred by TM7x to its host bacterium and further emphasizing the context-dependent nature of symbiotic relationships (41, 42). Intriguingly, our data showed that, when TM7x is associated with its host bacterium, the expression of ADS genes is relatively stable and not significantly influenced by the presence of arginine or acid stress (*SI Appendix*, Fig. S4). It is possible that the acquisition and catabolism of arginine via the ADS is important, not only for TM7x but also for its bacterial host (XH001) to cope with frequent acid stress in the oral cavity (Figs. 2 and 4). Thus, it may be advantageous to keep ADS expression constitutive. However, further study is required to test ADS expression under more diverse conditions, including those mimicking in vivo conditions, to fully understand the regulation of the ADS and its importance in XH001–TM7x symbiosis.

Host range is a key determinant of coevolutionary interactions between symbionts and their hosts (43). The observation that TM7x established successful epibiotic interaction only with *Actinomyces* spp. lacking an intact ADS pathway (Fig. 4) raised the intriguing question of whether ADS function plays a role in the coevolution of TM7x and its *Actinomyces* hosts, which warrants further investigation. The detailed mechanism governing the transition of Saccharibacteria from free-living cell to symbiont is still an unexplored question, and evolutionary events leading to the diversification of ADS function within the *Actinomyces* group remain to be determined. Nevertheless, the particular benefit provided by TM7x to its host bacterium via an encoded ADS pathway could likely contribute to the host selection and maintenance of cooperative epibiotic interaction with its hosts.

The catabolism of arginine via the ADS is a major contributor to the alkalinity of the oral microbiome, particularly the dental plaque microbiome due to the generation of ammonia, which is fundamental for maintaining heathy conditions and pH homeostasis (19, 40, 44). Clinical studies demonstrated that caries-free individuals have higher levels of ADI activity compared with individuals with active caries, suggesting that this pathway plays an important role in caries protection (45, 46). While the role of TM7x in maintaining pH homeostasis remains to be determined for the mouth, the TM7x-encoded ADS clearly has a significant effect on its persistence and that of the oral *Actinomyces* spp. with which it associates. Therefore, further study of the TM7x-encoded ADS in the oral cavity is warranted to better understand not only how it impacts its bacterial hosts' physiology and persistence but also how it modulates the structure and ecology of the oral microbiome.

Intriguing questions that remain to be further explored are the origins and timing of acquisition of the ADS by mammalian Saccharibacteria. Our data showed that, outside of the Saccharibacteria G1, the TM7x-encoded ADS displays the highest amino acid identity to that carried by HMT-350, a G6 Saccharibacteria. Genome-based analyses indicated that mammalian acquisition of the Saccharibacteria G1 (including TM7x) from an environmental source was likely a more recent event than that of G2 to G6 (7). Further, the ArcA enzyme encoded by mammal-associated Saccharibacteria G1 is more similar to phylogenetically distant Saccharibacteria (G6) than to more closely related environmental Saccharibacteria G1 (Fig. 1*D* and *SI Appendix*, Fig. S3). Thus, although we cannot completely rule out the possibility of ADS acquisition by TM7x before habitat transition, it is likely that TM7x or G1 Saccharibacteria may have acquired their ADS from mammalian G2 to G6 following their transition from environments. Intriguingly, when compared with those non-Saccharibacteria, the ADS operon from G1 and G6 displays the same gene arrangement as well as the highest amino acid identity to that carried by *Bacillus* spp., including *B. cereus* (Fig. 1*C* and *SI Appendix*, Fig. S2). *Bacillus* spp. is a group of facultative anaerobic gram-positive environmental bacteria, but can also transiently pass through the mammalian gastrointestinal tract and be present in the stools of healthy humans at varying levels (47). Such a transient interaction may have been sufficient to allow for Saccharibacterial acquisition of the ADS. Thus, the origin of the Saccharibacterial ADS, particularly for those non-G1, as well as the timing of acquisition, for example before or after their transition from the environment to mammals, remains an open question. Nevertheless, our experimental data fully support that the acquisition of the ADS provides a fitness advantage such that the majority of mammal-associated Saccharibacteria groups maintain this operon.

The ubiquity of Saccharibacteria within the human oral microbiome as well as the staggering microbial diversity and complexity of CPR bacteria present in host-associated and environmental microbiomes highlight the need for a better understanding of these understudied ultrasmall, bacterial lineages with highly reduced genomes. Our study provides experimental evidence demonstrating the benefit conferred by an acquired pathway (e.g., the ADS) in Saccharibacteria that not only helped facilitate their adaptation from the environment to mammals and is critical for them to maintain infectivity when disassociated from their host bacteria but may also contribute to the maintenance of cooperative episymbiotic interaction with their bacterial hosts, thus expanding the existing knowledge of these enigmatic bacterial lineages.

Materials and Methods

Phylogenomic Tree Reconstruction. Assemblies were derived from McLean et al. (7), and downloaded from PATRIC (48, 49) and the National Center for Biotechnology Information (NCBI). From PATRIC, a total of 96 genomes were selected based on genome completeness, contamination, and total contig number. With the genomes that met these criteria, the phylogenomic coverage across mammals, humans, and environment was the final criterion for the genomic tree construction. Phylogenetic analysis was carried out on 93 Saccharibacteria genomes that met the inclusion criteria. Three publicly available CPR genomes including Gracilibacteria (GN02), Kazan, and Absconditabacteria (SR-1) were used as outgroups. A total of 21 single-copy genes were then concatenated, aligned with MAFFT (12,726 aligned amino acids), and used to construct the phylogeny using methods previously described (7). Concatenated and aligned trees were inferred using RAxML (version 8.2.11) with the following commands: best tree and perform "fast bootstrapping". raxmlHPC-PTHREADS-SSE3 -s 96_genomes.phy -n 96_genomes -m GTRCAT -q 96_genomes.partitions -p 12345 -T 12 -f a -x 12345 -N 100. Genome trees from the RAxML output were annotated using Evolview (50). The detection of ADS genes was performed using PATRIC protein family annotations and these counts were aggregated for each assembly and included in the tree annotations along with the assembly source information (*SI Appendix*, Fig. S1).

Identification and Comparison of ADS Genes. To compare ADS operon structure between genomes, we downloaded publicly available genomes from the NCBI for *N. lyticus* TM7x, Saccharibacterium HMT-350 SAG1, *B. cereus* ATCC14579, *L. fermentum* IFO3956, *S. sanguinis* SK36, *S. pneumoniae* ATCC700669, and *A. johnsonii* F0510. The *A. johnsonii* F0510 genome was highly fragmented, consisting of 324 scaffolds, and thus the specific location of genes in this genome, namely the arginine/ornithine antiporter *arcD* being found separate from *arcABC*, should be interpreted with caution. The existing NCBI PGAP annotations were combined with eggNOG, Pfam, and TIGRFAM annotations to manually identify the *arcABC* operons. Windows containing a few genes upstream of the ADS operon(s) were extracted with a custom Python script. Gene arrangements were plotted with Clinker using default parameters (51). The predicted *arcD* found in the *A. johnsonii* genome was further assessed by BLAST search against NCBI's nr (nonredundant) database, revealing its closest hits were to known arginine/ornithine antiporters. This confirmed that our method indeed identified a true arginine/ornithine antiporter in *A. johnsonii*, although the draft quality of the genome prevented its confident localization.

Among these seven bacteria, amino acid sequences for the genes' ADS operon were aligned with MUSCLE (52) and the resultant percent identity was plotted as a heatmap in R. Note that MUSCLE employs a slightly different alignment algorithm from Clinker.

ArcA Phylogeny. All bacterial ArcA sequences on UniProtKB were downloaded by searching the following HAMAP-based query 'taxonomy:"Bacteria [2]" database:(type:hamap mf_00242)' in the UniProtKB search bar on 3 May 2021. This resulted in 8,892 ArcA sequences, including 29 sequences from Saccharibacteria. The 8,892 sequences were reduced to 279 representative sequences by clustering at 65% amino acid identity with CD-HIT (53). All Saccharibacteria ArcA sequences were readded to the 279 sequences, resulting in 304 sequences, which were used to reconstruct the ArcA phylogeny with RAxML (version 8.2.12) with the following commands: raxmlHPC-PTHREADS-AVX -p 123456 -x 123456 -f a -s arcA_tm7_uniprot-MUSCLE-uniq.faa -n arcA_tm7 -m PROTGAMMALG -N 300 -T 6. The tree was visualized with FigTree version 1.4.4. For the condensed tree, all parameters were identical except sequences were clustered at 50% identity and only a subset of Saccharibacteria sequences were added.

Bacteria Strains and Growth Conditions. TM7x (*N. lyticus* type, strain TM7x HMT-952) was previously coisolated together with its host bacterium *A. odontolyticus* subsp. *Actinosynbacter* strain XH001 (referred to as XH001) from the human oral cavity and can be maintained in Bacto brain heart infusion (BHI; BD) culture together with XH001 (referred to as XH001/TM7x coculture) (9). Our previous study showed that the coculture was heterogeneous and contained TM7x-associated, as well as TM7x-free, XH001 cells. XH001 was isolated from the coculture and maintained as XH001 monoculture (9), while XH001n was previously independently isolated from the same human subject and cultured without TM7x in the laboratory (11). Before each experiment, about 100-μL frozen stocks of XH001, XH001n, monoculture, or XH001/TM7x coculture were inoculated into 1 mL of BHI and incubated at 37 °C in a microaerophilic chamber (2% oxygen, 5% carbon dioxide, balanced with nitrogen). The cultures were then passaged once into 9 mL fresh BHI after 24-h incubation, followed by a second passage into 100 mL BHI before each experiment to keep homogeneity. *A. johnsonii* F0510, *A. graevenitzii* F0530, and *A. meyeri* W712 used in this study were grown in the same way as XH001.

Isolation of TM7x from XH001/TM7x Coculture. About 400 mL BHI-grown, maximum–cell density XH001/TM7x cocultures were separated into new 50-mL tubes and thoroughly vortexed to get as much free-floating TM7x as possible. The cocultures were then centrifuged at 5,000 × *g* for 10 min to pellet host cells and attached TM7x. The supernatant was filtrated through 0.45-μm Stericups (150 mL; Millipore) using house vacuum. The filtered supernatant was transferred into six 70-mL ultracentrifuge tubes (38 × 102 mm; Beckman) which fit a 45 Ti rotor. The tubes and 45 Ti rotor were then put into the ultracentrifuge machine (Optima L-80 XP; Beckman) and centrifuged at 80,000 × *g* for 1 h at 4 °C. Pelleted TM7x cells were resuspended and collected using 1 mL 145.5 mM NaCl (0.85% [weight/volume; wt/vol] NaCl, referred to as saline). We visually confirmed isolated free-floating TM7x cells using phase-contrast microscopy; at the same time, 50 μL resuspended cultures was plated on a BHI blood agar plate (with 5% sheep blood) and incubated at 37 °C in a microaerophilic chamber for 3 d to ensure there were no host cells. TM7x cells were centrifuged again in a tabletop centrifuge at 17,000 × *g* for 20 min at 4 °C for subsequent use.

TM7x-Encoded ADS Function Characterization. Isolated TM7x cells were washed twice using 1 mL saline to get rid of BHI carryover and resuspended with 10 mL saline, and then incubated at 37 °C in a microaerophilic chamber for 24 h to mimic starvation conditions and allow the intracellular carryover arginine to become fully catabolized. Twenty-four hours later, the TM7x cells were pelleted and resuspended in 12 mL saline supplemented with 10 mM L-arginine monohydrochloride (referred to as L-arginine in the text) and separated into three tubes with same amount of TM7x cells in each tube. The baseline 0-h intracellular citrulline, intracellular ATP, and extracellular ammonia were measured using a Citrulline Fluorometric Assay Kit (K2002-100; BioVision), ATP Colorimetric/Fluorometric Assay Kit (K354-100; BioVision), and Ammonia Assay Kit (AA0100; Sigma-Aldrich), respectively, according to each kit's protocol. The extracellular pH was also measured. After 2-h incubation in saline supplemented with arginine at 37 °C in a microaerophilic chamber, the intracellular citrulline, intracellular ATP, extracellular ammonia, and extracellular pH were measured again.

ADI Enzyme Inhibition Assay. TM7x cells were isolated and washed with saline, and then resuspended in stabilizing agent (50 mM Tris·HCl, 24% [wt/vol] sucrose, 10 mM $MgCl_2$, pH 7). The TM7x cell suspension was subjected to bead beating for 1 min. Lysozyme was added to the sample to a final concentration of 5 mg/mL and the sample was incubated for 1 h to further lyse the cells. The sample was centrifuged at 17,000 × *g* for 15 min at 4 °C to remove unbroken TM7x cells, lipids, and particulate matter, and the supernatant (e.g., lysate) was then transferred to a new tube and kept on ice; 90 μL lysate containing ADS enzymes was used to catalyze 3 mM L-arginine (control group) or 3 mM L-arginine supplemented with 3 mM L-canavanine (inhibitor group). Each reaction also contained 50 mM acetate buffer (pH 5.5) and 0.125% (wt/vol) sodium azide. After being incubated at 37 °C for 2 h, the reaction mixture was passed through a 10-kDa molecular weight cutoff spin column (BioVision; 1997) by centrifugation at 10,000 × *g* at 4 °C for 20 min. The ammonia concentration of the filtrate was measured using an Ammonia Assay Kit (AA0100; Sigma-Aldrich) according to the kit's protocol.

Pretreatment of TM7x for Cell-Membrane Integrity and Infectivity Assay. Isolated TM7x cells were washed twice using 1 mL saline to get rid of BHI carryover and separated into new tubes with the same amount of TM7x in each tube. One group of TM7x cells was resuspended in saline, and the other group of TM7x cells was resuspended in saline supplemented with 10 mM L-arginine monohydrochloride. TM7x cells in both groups were then incubated at 37 °C in a microaerophilic chamber. At day 1 and 7 time points, the same amount of TM7x cells was taken out from the two groups and centrifuged in a tabletop centrifuge at 17,000 × *g* for 20 min at 4 °C to collect TM7x cells for SYTOX Green staining and imaging (as described in the following section). Furthermore, at day 1, 2, and 7 time points, the same amount of TM7x cells was collected for SYTOX Green Stain quantitative analysis. The same amounts of TM7x from each group at the 24-h time point were taken for the infectivity assay.

Pretreatment of TM7x for Acid Stress Assay. Isolated TM7x cells were washed twice using 1 mL saline to get rid of BHI carryover and separated into new tubes with the same amount of TM7x in each tube. TM7x cells were then resuspended in pH 5 acetate buffer, pH 6 phosphate buffer, pH 7 phosphate buffer, and pH 5 acetate buffer supplemented with 10 mM L-arginine monohydrochloride, and then incubated at 37 °C in a microaerophilic chamber. At the 24-h time point, the same amount of TM7x cells was taken from the four groups and centrifuged in a tabletop centrifuge at 17,000 × *g* for 20 min at 4 °C to acquire TM7x cells for SYTOX Green Stain imaging and quantitative analysis. Furthermore, at the 24- and 48-h time points, the same amount of TM7x cells was also taken for infectivity assays. Since ammonia production from catabolization of arginine can enhance the pH, we measured the final pH of the group containing pH 5 acetate buffer supplemented with 10 mM L-arginine monohydrochloride to ensure the ammonia production did not exceed the pH 5 acetate buffer's buffering capacity.

Determining TM7x Membrane Integrity Using SYTOX Green Stain. Pretreated TM7x cells were washed twice using saline and resuspended in saline before staining. SYTOX Green Nucleic Acid Stain (5 μM; S7020; Invitrogen) was added to each tube to stain the cells for 15 min at room temperature while avoiding light. The TM7x cells were then washed twice using saline before being fixed with 4% formaldehyde for 3 h. Images were acquired by using a Zeiss LSM 880 confocal microscope under a 63× oil immersion objective with a 488-nm excitation laser. At least three fields of view per slide and three slides per tube were acquired.

Quantitative analysis of the SYTOX fluorescence intensity was carried out at days 1, 2, and 7. Approximately 5 μM SYTOX Green Nucleic Acid Stain (S7020; Invitrogen) was added to each tube containing saline-washed TM7x cells and separated into a 96-well black flat-bottom plate with 100 μL in each

well. The cells were stained for 15 min at room temperature while avoiding light. The 96-well plate was then read by a SpectraMax i3x microplate reader with SoftMax Pro software (version 7.0.3). The excitation and emission wavelengths were 488 and 523 nm. Several control wells with only saline and TM7x (free of SYTOX Green Stain) were used to deduct autofluorescence. Triton X-100 (1%; wt/vol) detergent–treated TM7x cells were used as positive controls in both the imaging and quantitative analysis procedure in Fig. 2.

TM7x Infectivity Assay. XH001n monocultures were grown in BHI until the second passage, and then aliquoted into new tubes with each tube containing 200 μL of $OD_{600\ nm}$ 0.4 cultures. The cells were pelleted by centrifugation at 17,000 × *g* for 5 min at 4 °C and resuspended in 200 μL of fresh BHI. To each tube of XH001n, different conditions or different amounts of pretreated TM7x were added. For the negative controls, we added cell-free saline; 0-h baseline controls were also set up using the same amount of freshly isolated TM7x cells. The XH001n and TM7x mixtures were incubated for 10 min at room temperature to allow TM7x to better attach onto XH001n before bringing the final volume to 2.5 mL using BHI. Cultures were incubated at 37 °C in a microaerophilic chamber, and we passaged the cultures every 24 h until the 10th passage. During each passage, we kept the initial $OD_{600\ nm}$ (0.1) and culture volume (2.5 mL) consistent by transferring the cultures into fresh BHI. The optical cell density of the cultures was monitored at 600 nm ($OD_{600\ nm}$) using a Spectronic Genesys 5 spectrophotometer to reflect XH001n growth conditions. For CFU data in Fig. 2*C*, the total CFU/mL was quantified by plating the cultures on a BHI agar plate and counting the colony numbers after 3 d of growth at 37 °C in a microaerophilic chamber. We carried out the infectivity assay in triplicate for both $OD_{600\ nm}$ measurement and CFU counting.

XH001/TM7x Coculture Acid Stress Assay. After growth in BHI until the second passage, XH001 monoculture and XH001/TM7x coculture were observed under the microscope to ensure the cells grew well. The cultures were harvested using a tabletop centrifuge at 7,800 rpm for 15 min at 4 °C and washed with saline once. Washed cells were resuspended in the following two different solutions with a final $OD_{600\ nm}$ of 0.5: 1) saline supplemented with 10 mM glucose, and 2) saline supplemented with 10 mM glucose and 10 mM L-arginine monohydrochloride. Solutions with XH001 or XH001/TM7x were incubated at 37 °C in a microaerophilic chamber. Samples were collected at the indicated time points to determine pH, ammonia production, as well as XH001 viability. Briefly, extracellular ammonia concentration was quantified at 0, 8, 16, and 24 h using the Ammonia Assay Kit (AA0100; Sigma-Aldrich) according to the manufacturer's instructions. pH was determined at 0.5, 1, 2, 4, 8, 12, 16, 20, and 24 h using a pH meter (Thermo Fisher). XH001 cell viability within XH001 monoculture and XH001/TM7x coculture was measured using a CFU assay: Duplicate samples taken at 0, 4, 8, 12, 16, 20, and 24 h were serially diluted and plated onto BHI blood agar plates (with 5% sheep blood) (11). Plate serial dilution was performed at 0, 10^{-1}, 10^{-2}, 10^{-3}, 10^{-4}, and 10^{-5} with a 10-μL spot, and then incubated at 37 °C in a microaerophilic chamber for at least 3 d before CFU counting. All the assays were performed with two technical replicates and two biological replicates.

TM7x Host Range, *Actinomyces* Phylogeny, and Association with the ADS. We previously downloaded and analyzed the genomes of 23 *Actinomyces* spp. (28). From these genomes, ADS genes were identified using a combination of annotations including Enzyme Commission numbers, eggNOG, Pfam, and TIGRFAM as described above to generate a matrix of ADS presence/absence for each genome. A phylogenomic tree was also created with PhyloPhlAn version 3 as described in Utter et al. (28) with an outgroup of *Pseudopropionibacterium propionicum* F0700, *Corynebacterium durum* F0235, and *Corynebacterium matruchotii* NCTC10206 genomes downloaded from the NCBI. Briefly, PhyloPhlAn uses concatenated core genes to construct a maximum likelihood–based tree. The phylogenomic tree was then plotted and combined with ADS gene presence/absence with a custom R script.

Data Availability. All study data are included in the article and/or *SI Appendix*.

ACKNOWLEDGMENTS. We thank Dr. Felicitas Bidlack and Dr. Pallavi Murugkar at The Forsyth Institute for assisting with acquisition of scanning electron microscopy images. We thank Dr. Fabian Schulte at Brandeis University for insightful discussions. Research in this publication was supported by the National Institute of Dental and Craniofacial Research of the NIH under Awards 1R01DE023810, 1R01DE020102, and 1R01DE026186 (to X.H., J.S.M., and W.S.) and F32DE025548-01 and 1K99DE027719-01 (to B.B.). The content is solely the responsibility of the authors and does not necessarily represent the official views of the NIH.

1. C. J. Castelle, J. F. Banfield, Major new microbial groups expand diversity and alter our understanding of the tree of life. *Cell* **172**, 1181–1197 (2018).
2. L. A. Hug *et al.*, A new view of the tree of life. *Nat. Microbiol.* **1**, 16048 (2016).
3. D. H. Parks *et al.*, A standardized bacterial taxonomy based on genome phylogeny substantially revises the tree of life. *Nat. Biotechnol.* **36**, 996–1004 (2018).
4. C. T. Brown *et al.*, Unusual biology across a group comprising more than 15% of domain Bacteria. *Nature* **523**, 208–211 (2015).
5. A. Shaiber *et al.*, Functional and genetic markers of niche partitioning among enigmatic members of the human oral microbiome. *Genome Biol.* **21**, 292 (2020).
6. A. L. Jaffe *et al.*, Pattern of gene content and co-occurrence constrain the evolutionary path toward animal association in CPR bacteria. *mBio.* **12**, e0052121 (2021).
7. J. S. McLean *et al.*, Acquisition and adaptation of ultra-small parasitic reduced genome bacteria to mammalian hosts. *Cell Rep.* **32**, 107939 (2020).
8. C. He *et al.*, Genome-resolved metagenomics reveals site-specific diversity of episymbiotic CPR bacteria and DPANN archaea in groundwater ecosystems. *Nat. Microbiol.* **6**, 354–365 (2021).
9. X. He *et al.*, Cultivation of a human-associated TM7 phylotype reveals a reduced genome and epibiotic parasitic lifestyle. *Proc. Natl. Acad. Sci. U.S.A.* **112**, 244–249 (2015).
10. B. Bor *et al.*, Phenotypic and physiological characterization of the epibiotic interaction between TM7x and its basibiont *Actinomyces*. *Microb. Ecol.* **71**, 243–255 (2016).
11. B. Bor *et al.*, Rapid evolution of decreased host susceptibility drives a stable relationship between ultrasmall parasite TM7x and its bacterial host. *Proc. Natl. Acad. Sci. U.S.A.* **115**, 12277–12282 (2018).
12. B. Bor *et al.*, Insights obtained by culturing Saccharibacteria with their bacterial hosts. *J. Dent. Res.* **99**, 685–694 (2020).
13. B. C. Van Wuyckhuyse *et al.*, Association of free arginine and lysine concentrations in human parotid saliva with caries experience. *J. Dent. Res.* **74**, 686–690 (1995).
14. I. M. Velsko, B. Chakraborty, M. M. Nascimento, R. A. Burne, V. P. Richards, Species designations belie phenotypic and genotypic heterogeneity in oral streptococci. *mSystems* **3**, e00158-18 (2018).
15. N. Takahashi, Oral microbiome metabolism: From "who are they?" to "what are they doing?" *J. Dent. Res.* **94**, 1628–1637 (2015).
16. Y. C. Luiking, G. A. M. Ten Have, R. R. Wolfe, N. E. P. Deutz, Arginine de novo and nitric oxide production in disease states. *Am. J. Physiol. Endocrinol. Metab.* **303**, E1177–E1189 (2012).
17. R. E. Marquis, G. R. Bender, D. R. Murray, A. Wong, Arginine deiminase system and bacterial adaptation to acid environments. *Appl. Environ. Microbiol.* **53**, 198–200 (1987).
18. M. Agnello *et al.*, Arginine improves pH homeostasis via metabolism and microbiome modulation. *J. Dent. Res.* **96**, 924–930 (2017).
19. R. A. Burne, R. E. Marquis, Alkali production by oral bacteria and protection against dental caries. *FEMS Microbiol. Lett.* **193**, 1–6 (2000).
20. H. J. Verhoogt *et al.*, arcD, the first gene of the arc operon for anaerobic arginine catabolism in *Pseudomonas aeruginosa*, encodes an arginine-ornithine exchanger. *J. Bacteriol.* **174**, 1568–1573 (1992).
21. N. Ivanova *et al.*, Genome sequence of *Bacillus cereus* and comparative analysis with *Bacillus anthracis*. *Nature* **423**, 87–91 (2003).
22. E. E. Noens, J. S. Lolkema, Convergent evolution of the arginine deiminase pathway: The ArcD and ArcE arginine/ornithine exchangers. *MicrobiologyOpen* **6**, e00412 (2017).
23. R. L. Wijeyeweera, I. Kleinberg, Arginolytic and ureolytic activities of pure cultures of human oral bacteria and their effects on the pH response of salivary sediment and dental plaque in vitro. *Arch. Oral Biol.* **34**, 43–53 (1989).
24. B. Xu *et al.*, The arginine deiminase system facilitates environmental adaptability of *Streptococcus equi* ssp. *zooepidemicus* through pH adjustment. *Res. Microbiol.* **167**, 403–412 (2016).
25. L. Li *et al.*, Inactivation of microbial arginine deiminases by L-canavanine. *J. Am. Chem. Soc.* **130**, 1918–1931 (2008).
26. J. W. Moulder, Comparative biology of intracellular parasitism. *Microbiol. Rev.* **49**, 298–337 (1985).
27. S. L. Russell, Transmission mode is associated with environment type and taxa across bacteria-eukaryote symbioses: A systematic review and meta-analysis. *FEMS Microbiol. Lett.* **366**, fnz013 (2019).
28. D. R. Utter, X. He, C. M. Cavanaugh, J. S. McLean, B. Bor, The saccharibacterium TM7x elicits differential responses across its host range. *ISME J.* **14**, 3054–3067 (2020).
29. R. M. Stephan, B. F. Miller, A quantitative method for evaluating physical and chemical agents which modify production of acids in bacterial plaques on human teeth. *J. Dent. Res.* **22**, 45–51 (1943).
30. P. D. Cotter, C. Hill, Surviving the acid test: Responses of gram-positive bacteria to low pH. *Microbiol. Mol. Biol. Rev.* **67**, 429–453 (2003).
31. J. P. Gogarten, J. P. Townsend, Horizontal gene transfer, genome innovation and evolution. *Nat. Rev. Microbiol.* **3**, 679–687 (2005).
32. G. Schönknecht *et al.*, Gene transfer from bacteria and archaea facilitated evolution of an extremophilic eukaryote. *Science* **339**, 1207–1210 (2013).
33. R. Niehus, S. Mitri, A. G. Fletcher, K. R. Foster, Migration and horizontal gene transfer divide microbial genomes into multiple niches. *Nat. Commun.* **6**, 8924 (2015).
34. S. M. Soucy, J. Huang, J. P. Gogarten, Horizontal gene transfer: Building the web of life. *Nat. Rev. Genet.* **16**, 472–482 (2015).

35. A. Levy *et al.*, Genomic features of bacterial adaptation to plants. *Nat. Genet.* **50**, 138–150 (2017).
36. S. K. Sheppard, D. S. Guttman, J. R. Fitzgerald, Population genomics of bacterial host adaptation. *Nat. Rev. Genet.* **19**, 549–565 (2018).
37. J. H. Hehemann *et al.*, Transfer of carbohydrate-active enzymes from marine bacteria to Japanese gut microbiota. *Nature* **464**, 908–912 (2010).
38. Y. Hirose *et al.*, *Streptococcus pyogenes* upregulates arginine catabolism to exert its pathogenesis on the skin surface. *Cell Rep.* **34**, 108924 (2021).
39. A. Edlund *et al.*, Meta-omics uncover temporal regulation of pathways across oral microbiome genera during in vitro sugar metabolism. *ISME J.* **9**, 2605–2619 (2015).
40. I. Kleinberg, A mixed-bacteria ecological approach to understanding the role of the oral bacteria in dental caries causation: An alternative to *Streptococcus mutans* and the specific-plaque hypothesis. *Crit. Rev. Oral Biol. Med.* **13**, 108–125 (2002).
41. R. M. Fisher, L. M. Henry, C. K. Cornwallis, E. T. Kiers, S. A. West, The evolution of host-symbiont dependence. *Nat. Commun.* **8**, 15973 (2017).
42. D. Lindell *et al.*, Transfer of photosynthesis genes to and from *Prochlorococcus* viruses. *Proc. Natl. Acad. Sci. U.S.A.* **101**, 11013–11018 (2004).
43. F. A. Gorter, A. R. Hall, A. Buckling, P. D. Scanlan, Parasite host range and the evolution of host resistance. *J. Evol. Biol.* **28**, 1119–1130 (2015).
44. N. Takahashi, B. Nyvad, Caries ecology revisited: Microbial dynamics and the caries process. *Caries Res.* **42**, 409–418 (2008).
45. M. M. Nascimento *et al.*, Oral arginine metabolism may decrease the risk for dental caries in children. *J. Dent. Res.* **92**, 604–608 (2013).
46. M. M. Nascimento, V. V. Gordan, C. W. Garvan, C. M. Browngardt, R. A. Burne, Correlations of oral bacterial arginine and urea catabolism with caries experience. *Oral Microbiol. Immunol.* **24**, 89–95 (2009).
47. L. P. Stenfors Arnesen, A. Fagerlund, P. E. Granum, From soil to gut: *Bacillus cereus* and its food poisoning toxins. *FEMS Microbiol. Rev.* **32**, 579–606 (2008).
48. J. J. Davis *et al.*, The PATRIC Bioinformatics Resource Center: Expanding data and analysis capabilities. *Nucleic Acids Res.* **48**, D606–D612 (2020).
49. T. Brettin *et al.*, RASTtk: A modular and extensible implementation of the RAST algorithm for building custom annotation pipelines and annotating batches of genomes. *Sci. Rep.* **5**, 8365 (2015).
50. B. Subramanian, S. Gao, M. J. Lercher, S. Hu, W. H. Chen, Evolview v3: A webserver for visualization, annotation, and management of phylogenetic trees. *Nucleic Acids Res.* **47**, W270–W275 (2019).
51. C. L. M. Gilchrist, Y. H. Chooi, Clinker & clustermap.js: Automatic generation of gene cluster comparison figures. *Bioinformatics*, 10.1093/bioinformatics/btab007 (2021).
52. R. C. Edgar, MUSCLE: Multiple sequence alignment with high accuracy and high throughput. *Nucleic Acids Res.* **32**, 1792–1797 (2004).
53. L. Fu, B. Niu, Z. Zhu, S. Wu, W. Li, CD-HIT: Accelerated for clustering the next-generation sequencing data. *Bioinformatics* **28**, 3150–3152 (2012).